Electroweak boson production in double parton scattering

Krzysztof Golec-Biernat*
Institute of Nuclear Physics Polish Academy of Sciences, 31-342 Cracow, Poland and
Faculty of Mathematics and Natural Sciences, University of Rzeszów, 35-959 Rzeszów, Poland

Emilia Lewandowska†
Institute of Nuclear Physics Polish Academy of Sciences, 31-342 Cracow, Poland

We study the W^+W^- and Z^0Z^0 electroweak boson production in double parton scattering using QCD evolution equations for double parton distributions. In particular, we analyze the impact of splitting terms in the evolution equations on the double parton scattering cross sections. Unlike the standard terms, the splitting terms are not suppressed for large values of the relative momentum of two partons in the double parton scattering. Thus, they play an important role which we discuss in detail for the single splitting contribution to the cross sections under the study.

Keywords: quantum chromodynamics, double parton scattering, double parton distributions evolution equations, electroweak bosons

arXiv:1407.4038v2 [hep-ph] 6 Nov 2014

I. INTRODUCTION

The double parton scattering (DPS) in high-energy hadron scattering is a process in which two hard interactions with large scales (much bigger that nucleon mass) take place in one scattering event. Such a process is usually interpreted in QCD as scattering of two pairs of partons (quarks or gluons) from incoming hadrons. The DPS is the simplest multiparton process with hard scales which allows one to gain information on parton correlations inside hadrons. Thus, it has been studied for many years from both theoretical [1–19] and phenomenological sides [20–36]. The experimental evidence of the DPS from Tevatron and the LHC has been presented in [37–43]. At the LHC, the DPS is crucial for a better understanding of background for many important processes, e.g. the Higgs boson production [21, 44], as well as for a better description of multiparton interactions needed for modeling the underlying event, see Refs. [25, 32]. It is, therefore, very important to use a rigorous approach to the DPS which is based on QCD.

The inclusive DPS cross section in the collinear approximation takes the form [15]

$$\sigma_{AB} = \frac{N}{2}\sum_{f_1f_2f_1'f_2'}\int dx_1dx_2\,dz_1dz_2\,\frac{d^2\mathbf{q}}{(2\pi)^2} \times D_{f_1f_2}(x_1,x_2,Q_1,Q_2,\mathbf{q})\,\hat{\sigma}^A_{f_1f_1'}(Q_1)\,\hat{\sigma}^B_{f_2f_2'}(Q_2)\,D_{f_1'f_2'}(z_1,z_2,Q_1,Q_2,-\mathbf{q}), \quad (1)$$

where A and B denote two final states from two parton interactions with hard scales $Q_i = x_iz_i\sqrt{s}$, where $\sqrt{s}$ is center-of-mass energy of the colliding hadrons. In addition, N is a symmetry factor, equal to 1 for $A = B$ and 2 otherwise, and $D_{f_1f_2}(x_1,x_2,Q_1,Q_2,\mathbf{q})$ are the *collinear* double parton distribution functions (DPDFs) in a hadron, see Fig. 1 for schematic illustration. They depend on parton longitudinal momentum fraction $x_{1,2}$ and parton flavors $f_{1,2}$, two hard scales $Q_{1,2}$, and a relative transverse momentum $\mathbf{q}$. The latter momentum is related to the momentum structure of four parton fields in the definition of unintegrated DPDFs, see [15] for more details. The momentum fractions obey the condition

$$0 < x_1 + x_2 \le 1\,, \quad (2)$$

which means that the sum of parton longitudinal momenta cannot exceed the total nucleon momentum. This is the basic parton correlation which has to be taken into account. For more advanced aspects of parton correlations see Refs. [15, 16].

We start from the cross section formula in which the DPDFs depend on exchange momentum $\mathbf{q}$ rather than on the Fourier conjugate variable $\mathbf{b}$, being interpreted as transverse distance between two partons taking part in hard

*Electronic address: golec@ifj.edu.pl
†Electronic address: emilia.lewandowska@ifj.edu.pl

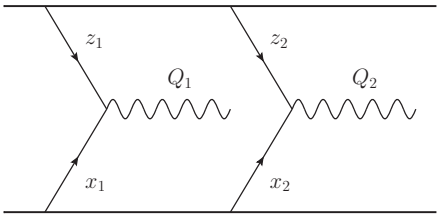

FIG. 1: Example of double parton scattering.

scattering. The latter possibility as a starting point creates more problems than answers [10, 15], despite its apparent attractiveness for phenomenological modeling of the DPDF dependence on this variable.

The DPDFs obey QCD evolution equations known at present in the leading logarithmic approximation [1, 2, 5, 6, 45]. These are the Dokshitzer-Gribov-Lipatov-Altarelli-Parisi (DGLAP)-type evolution equations with additional nonhomogeneous terms which describe splitting of a single parton into two partons. The role of these terms for the DPS cross section predictions is the main subject of this paper. We will focus on the electroweak boson production which is one of the cleanest processes for such an analysis. The electroweak bosons are color singlets, thus the collinear factorization formula (1) is not endangered by soft gluon final state interactions which might break factorization.

The paper is organized as follows. In Sec. II we describe evolution equations the DPDFs in the leading logarithmic approximation. In Sec. III we derive the general solution to these equation in the Mellin moment space while in Sec. IV we present assumptions concerning the relative momentum dependence of the DPDFs. In Sec. V we apply the presented results to the computation of the electroweak boson production cross sections and in Sec. VI we discuss the role of the contributions with the splitting terms. We conclude with a summary of our findings.

II. EVOLUTION EQUATIONS FOR DPDFS

Evolution equations for the DPDFs are known in the leading logarithmic approximation (LLA) in which large powers of $(\alpha_s \ln(Q^2/\Lambda^2))^n$ are resumed to all orders in n. They were derived in [1, 2, 5, 6] for equal hard scales, $Q_1 = Q_2 \equiv Q$, and for the relative momentum $\mathbf{q} = 0$,

$$\begin{aligned}\partial_t D_{f_1 f_2}(x_1, x_2, t) \;=\; & \sum_{f'} \int_{x_1}^{1-x_2} \frac{du}{u}\, P_{f_1 f'}\Big(\frac{x_1}{u}\Big)\, D_{f' f_2}(u, x_2, t) \\ & + \sum_{f'} \int_{x_2}^{1-x_1} \frac{du}{u}\, P_{f_2 f'}\Big(\frac{x_2}{u}\Big)\, D_{f_1 f'}(x_1, u, t) \\ & + \frac{1}{x_1 + x_2} \sum_{f'} P_{f' \to f_1 f_2}\left(\frac{x_1}{x_1 + x_2}\right) D_{f'}(x_1 + x_2, t)\,, \end{aligned} \tag{3}$$

where we absorbed the leading order strong coupling constant into the definition of the evolution parameter,

$$t \;\equiv\; t(Q) \;=\; \int_{Q_0^2}^{Q^2} \frac{\alpha_s(\mu^2)}{2\pi} \frac{d\mu^2}{\mu^2}\,, \tag{4}$$

and introduced the shorthand notation for the DPDFs:

$$D_{f_1 f_2}(x_1, x_2, t) \equiv D_{f_1 f_2}(x_1, x_2, Q, Q, \mathbf{q} = 0)\,. \tag{5}$$

Notice that $t = 0$ corresponds to an initial scale Q_0 at which the parton distributions need to be specified. The first discussion of next-to-leading corrections to these equations can be found in [7, 9]. The integral kernels in Eq. (3) are the leading order Altarelli-Parisi splitting functions, with virtual corrections included, which describe the splitting of one of the two partons, while the remaining parton stays intact. This gives the upper integration limits resulting from condition (2).

The last term on the rhs of Eq. (3), called from now on the *splitting term*, describes the real splitting of parton f' into two given partons f_1 and f_2. The functions $P_{f' \to f_1 f_2}$ are directly related to the real emission Altarelli-Parisi splitting functions in the LLA, $P^{(0)}_{f'f}$. In particular, we have

$$P_{q\to qg}(z) = P^{(0)}_{qq}(z)\,, \quad P_{q\to gq}(z) = P^{(0)}_{qg}(z)\,, \quad P_{g\to q\overline{q}}(z) = P^{(0)}_{gq}(z)\,, \quad P_{g\to gg}(z) = P^{(0)}_{gg}(z)\,. \tag{6}$$

The single parton distributions, $D_{f'}(x_1+x_2,t)$, which appear in the splitting term, provide an additional dependence on t in Eq. (3), imposed by the DGLAP evolution equations,

$$\partial_t D_f(x,t) = \sum_{f'} \int_x^1 \frac{du}{u}\, P_{ff'}\Big(\frac{x}{u}\Big)\, D_{f'}(u,t). \tag{7}$$

The impact of the splitting terms on the DPS cross sections is the main subject of our paper.

III. SOLUTION TO EVOLUTION EQUATIONS

Evolution equations (3) greatly simplify in the space of Mellin moments, obtained after the double Mellin transform of the DPDFs with respect to the momentum fractions $x_{1,2}$ which obey condition (2) imposed by the step function $\Theta(1-x_1-x_2)$,

$$\tilde{D}_{f_1f_2}(n_1,n_2,t) = \int_0^1 dx_1 \int_0^1 dx_2\, x_1^{n_1}\, x_2^{n_1}\, \Theta(1-x_1-x_2)\, D_{f_1f_2}(x_1,x_2,t). \tag{8}$$

Introducing the matrix notation with respect to parton flavors (including gluon), $\tilde{D} = (\tilde{D}_{f_1f_2})$, we find the new form of Eq. (3):

$$\partial_t \tilde{D}(n_1,n_2,t) = \gamma(n_1)\, \tilde{D}(n_1,n_2,t) + \tilde{D}(n_1,n_2,t)\, \gamma^T(n_2) \,+\, \tilde{\gamma}(n_1,n_2)\, \tilde{D}(n_1+n_2,t) \tag{9}$$

where

$$\gamma(n) = \int_0^1 dx\, x^n P(x)\,, \qquad\qquad \tilde{\gamma}(n_1,n_2) = \int_0^1 dx\, x^{n_1}(1-x)^{n_2} P(x) \tag{10}$$

are known matrices of anomalous dimensions and $\tilde{D}(n_1+n_2,t)$ is a vector of the Mellin moments of the SPDFs,

$$\tilde{D}_f(n,t) = \int_0^1 dx\, x^n\, D_f(x,t)\,. \tag{11}$$

They obey the DGLAP equation (7) in the Mellin moment space,

$$\partial_t \tilde{D}(n,t) \;=\; \gamma(n)\, \tilde{D}(n,t)\,. \tag{12}$$

Equation (9) is a nonhomogeneous first order linear differential equation. Thus, its solution is the sum of the general solution to the homogeneous equation (without the splitting term) and a particular solution to the nonhomogeneous equation. The homogeneous equation has the following general solution:

$$\tilde{D}(n_1,n_2,t) \;=\; \mathrm{e}^{\gamma(n_1)\,t}\, A(n_1,n_2)\, \mathrm{e}^{\gamma^T(n_2)\,t}\,, \tag{13}$$

where the exponentials generate two DGLAP evolutions since the solution to Eq. (12) reads

$$\tilde{D}(n,t) \;=\; \mathrm{e}^{\gamma(n)\,t} \tilde{D}_0(n) \tag{14}$$

where $\tilde{D}_0(n)$ is an initial condition. A particular solution to Eq. (9) can now be found by making $A(n_1,n_2)$ time dependent. Substituting such an ansatz to Eq. (13), we find the equation

$$\partial_t A(n_1,n_2,t) \;=\; \mathrm{e}^{-\gamma(n_1)\,t}\, \tilde{\gamma}(n_1,n_2)\, \tilde{D}(n_1+n_2,t)\, \mathrm{e}^{-\gamma^T(n_2)\,t} \tag{15}$$

which can be easily solved:

$$A(n_1,n_2,t) \;=\; \tilde{D}_0(n_1,n_2) \;+\; \int_0^t dt'\, \mathrm{e}^{-\gamma(n_1)\,t'}\, \tilde{\gamma}(n_1,n_2)\, \tilde{D}(n_1+n_2,t')\, \mathrm{e}^{-\gamma^T(n_2)\,t'}\,. \tag{16}$$

Thus, after substituting (16) in Eq. (13), we obtain the final form of the solution to the evolution equations:

$$\tilde{D}(n_1,n_2,t) = \mathrm{e}^{\gamma(n_1)\,t}\, \tilde{D}_0(n_1,n_2)\, \mathrm{e}^{\gamma^T(n_2)\,t} \;+\; \int_0^t dt'\, \mathrm{e}^{\gamma(n_1)(t-t')}\, \tilde{\gamma}(n_1,n_2)\, \tilde{D}(n_1+n_2,t')\, \mathrm{e}^{\gamma^T(n_2)(t-t')} \tag{17}$$

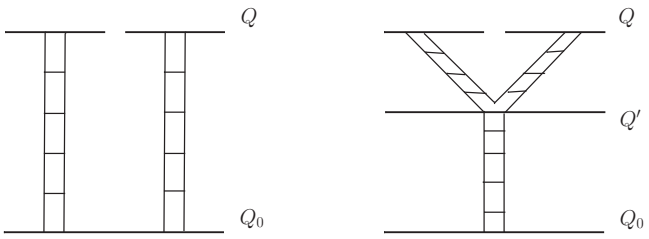

FIG. 2: Schematic illustration of the two contributions in solution (17).

where $\tilde{D}_0(n_1, n_2)$ is an initial condition at $t = 0$. Solution (17) is the sum of two terms, see also Fig. 2. The first term describes two independent DGLAP evolutions up to the scale Q [related to t by Eq. (4)] of two parton ladders emerging from a hadron at the initial scale Q_0 ($t = 0$). The second term describes the emergence of two parton ladders from a single parton ladder through the splitting at the scale Q' (corresponding to t') and their independently evolution up to the scale Q. Solution (17) can also be written in the x space using the inverse Mellin transform, see Ref. [46].

Notice that the first term in Eq. (17) is a solution to the homogeneous equation (9) without the splitting term, $\tilde{D}^{(hom)}$, which depends on the initial condition for the DPDFs, while the second term, which we denote by $\tilde{D}^{(nhom)}$, depends only on the initial condition for the SPDFs. Thus, it can be computed for any initial conditions for DPDFs as the difference between the solutions to the nonhomogeneous and the homogeneous equations. It can also be directly obtained by solving to the nonhomogeneous equation with zero initial conditions for DPDFs.

In Fig. 3 we plot the DPDFs for the indicated flavors as functions of x_1 for fixed $x_2 = 10^{-2}$ and $Q^2 = 10^3$ GeV^2. We see that for $x < 0.1$, the splitting part of the solution, $\tilde{D}^{(nhom)}$, is significantly smaller than $\tilde{D}^{(hom)}$ with the ratio of the order of 10^{-1}.

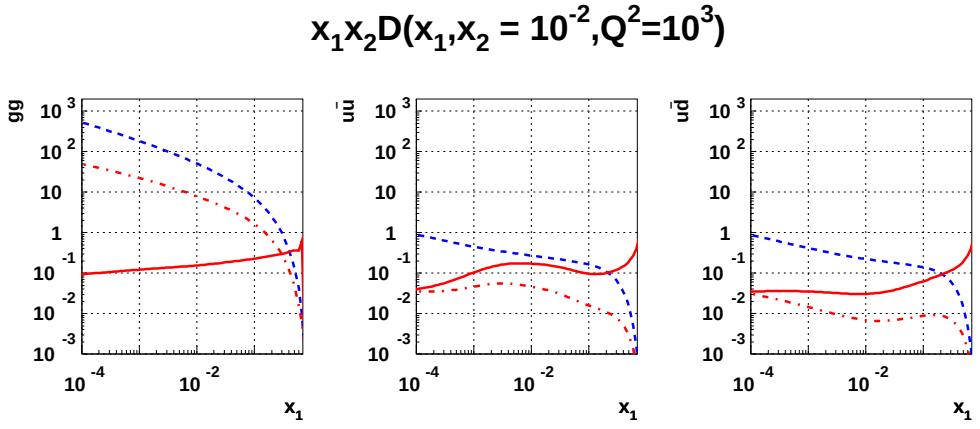

FIG. 3: The homogeneous, $\tilde{D}^{(hom)}$ (dashed lines), and nonhomogeneous, $\tilde{D}^{(nhom)}$ (dash-dotted lines), solutions for the indicated flavors. The ratios of the two solutions are shown as the solid lines.

The curves in Fig. 3, as well as the rest of the numerical results shown in this paper, were obtained with our numerical program [47] which solves evolution equations (3) and (7), using the Chebyshev polynomial expansion on the grid of Chebyshev nodes, $y_i \in [-1, 1]$, see [48] for more details. These nodes were subsequently transformed into the range appropriate for the parton distribution functions, $x \in [x_{\min}, 1]$, through the logarithmic transformation $y = A \ln x + B$. We used $N = 30$ nodes for $x_{\min} = 10^{-5}$, and 10 point grid for the variable t in the range corresponding to $Q \in [2, 200]$ GeV.

IV. RELATIVE MOMENTUM DEPENDENCE

The form (17) of the solution is the basis of the proposition of Ryskin and Snigirev [12] concerning the dependence of the DPDFs on the relative momentum $\mathbf{q}$. Such a dependence is not specified by the evolution equations and is

a matter of a physically motivated modeling. The basic idea is that for two partons originating from a nucleon, $\mathbf{q}$ reflects their correlation inside the nucleon described by a nonperturbative form factor. On the other hand, if the two partons originate from a pointlike parton through its splitting, the form factor no longer exists.

Therefore, the first term in Eq. (17) has been postulated in [12] with the factorized $\mathbf{q}$ dependence,

$$\tilde{D}^{(1)}(n_1,n_2,t,\mathbf{q}) \,=\, \mathrm{e}^{\gamma(n_1)\,t}\,\tilde{D}_0(n_1,n_2)\,\mathrm{e}^{\gamma^T(n_2)\,t}\,F_{2g}^2(\mathbf{q}) \tag{18}$$

where $F_{2g}(\mathbf{q})$ is the two-gluon nucleon form factor in the dipole form

$$F_{2g}(\mathbf{q}) \,=\, \frac{1}{\left(1+\mathbf{q}^2/m_g^2\right)^2} \tag{19}$$

and m_g is the effective gluon mass. In principle, the form factor could depend on parton flavors, however, this dependence is not taken into account.

In the second term in Eq. (17), the $\mathbf{q}$ dependence has been introduced through the lower integration limit,

$$\tilde{D}^{(2)}(n_1,n_2,t,\mathbf{q}) \,=\, \int_{t_0}^{t} dt'\,\mathrm{e}^{\gamma(n_1)(t-t')}\,\tilde{\gamma}(n_1,n_2)\,\tilde{D}(n_1+n_2,t')\,\mathrm{e}^{\gamma^T(n_2)(t-t')} \tag{20}$$

where

$$t_0 \,=\, \begin{cases} t(|\mathbf{q}|) & \text{if } \; Q_0<|\mathbf{q}|\le Q \\ \\ 0 & \text{if } \; |\mathbf{q}|\le Q_0 \end{cases} \tag{21}$$

and $t(|\mathbf{q}|)$ is given by Eq. (4). Thus, for $|\mathbf{q}|>Q_0$, $|\mathbf{q}|$ is the scale from which the splitting starts. For $|\mathbf{q}|<Q_0$, the relative loop momentum is small and may be neglected due to strong ordering in transverse parton momenta in the DGLAP ladder. In such a case, the integration in Eq. (20) starts from Q_0 which corresponds to $t_0=0$. The values of $|\mathbf{q}|$ were restricted to $|\mathbf{q}|\le Q$, which means that Q is the largest scale in the problem.

The two components given by Eqs. (18) and (20) can also be written in the x space, see [12]. In this way, the general form of the DPDFs reads

$$D(x_1,x_2,Q,\mathbf{q}) \,=\, D^{(1)}(x_1,x_2,Q,\mathbf{q}) \,+\, D^{(2)}(x_1,x_2,Q,\mathbf{q})\,, \tag{22}$$

where we reintroduced the hard scale Q in the notation [corresponding to $t=t(Q)$]. Cross section (1) can be written in terms of these components as the sum

$$\sigma_{AB} \,=\, \sigma_{AB}^{(11)} \,+\, \sigma_{AB}^{(12+21)} \,+\, \sigma_{AB}^{(22)} \tag{23}$$

where

$$\begin{aligned}\sigma_{AB}^{(ij)} \,=\, & \frac{N}{2}\sum_{f_i,f_i'}\int dx_1dx_2\,dz_1dz_2\int\frac{d^2\mathbf{q}}{(2\pi)^2}\,\theta(Q-|\mathbf{q}|) \\ & \times\; D_{f_1f_2}^{(i)}(x_1,x_2,Q,\mathbf{q})\,\hat{\sigma}_{f_1f_1'}^{A}(Q)\,\hat{\sigma}_{f_2f_2'}^{B}(Q)\,D_{f_1'f_2'}^{(j)}(z_1,z_2,Q,-\mathbf{q}).\end{aligned} \tag{24}$$

Notice that the integration over $\mathbf{q}$ is bounded from above by the hard scale Q. Each term in the above sum has a clear interpretation; $\sigma_{AB}^{(11)}$ is a contribution without parton splitting, $\sigma_{AB}^{(12+21)}$ is a single splitting contribution while $\sigma_{AB}^{(22)}$ is a double splitting contribution with two parton splittings from both hadrons each. The latter contribution was a matter of intensive debate in past years, see [10, 11, 14, 15, 18, 49], with a conclusion that it should rather be classified as the single parton scattering process since it is entirely driven by the SPDFs. However, it was advocated in Ref. [18] that the complete removal of the double splitting graphs from the DPS cross section is not the quite correct prescription. All this means that the double splitting contribution needs careful diagrammatic analysis. Thus, we do not consider the $\sigma_{AB}^{(22)}$ contribution in our forthcoming presentation, leaving the problem of the double splitting graphs to a separate analysis.

In the standard approach, the estimation of DPS cross sections is usually made with the formula

$$\sigma_{AB} \,=\, \frac{N}{2}\,\frac{\sigma_A\sigma_B}{\sigma_{\mathrm{eff}}}\,, \tag{25}$$

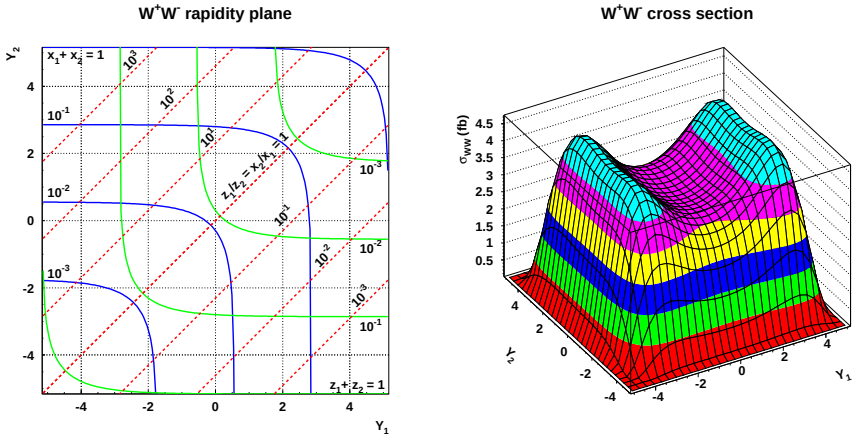

FIG. 4: Rapidity plane for W^+W^- boson production (left) and cross section (28) (in femtobarns) (right).

where σ_A and σ_B are the single parton scattering cross sections and $\sigma_{\rm eff}$ is an effective cross section, present here for the dimensional reason. The CDF and D0 collaborations estimated the value $\sigma_{\rm eff} \approx 15$ mb from the DPS dijet data [38–40]. Comparing (25) to the standard contribution $\sigma_{AB}^{(11)}$ we see that $\sigma_{\rm eff}$ is the inverse of the integral,

$$\int \frac{d^2\mathbf{q}}{(2\pi)^2}\,\theta(Q-|\mathbf{q}|)\,F_{2g}^4(\mathbf{q}) = \frac{m_g^2}{28\pi} \tag{26}$$

for $Q \gg m_g$, which leads to effective gluon mass $m_g \approx 1.5$ GeV.

V. ELECTROWEAK BOSON PRODUCTION IN DPS

As an application of the presented formalism, we consider the DPS electroweak boson production W^+W^- and Z^0Z^0 in the proton-proton scattering at the LHC center-of-mass energy $\sqrt{s} = 14$ TeV. The hard scale in this case is given by the boson mass, $Q = M_{W,Z}$. We compute the DPS cross section (24), $d^2\sigma_{AB}/dy_1dy_2$, differential in boson rapidities $y_{1,2}$. In such a case, in the collinear approach, the parton momentum fractions obey the condition

$$x_{1,2} = \frac{Q}{\sqrt{s}}\,{\rm e}^{y_{1,2}}\,, \qquad z_{1,2} = \frac{Q}{\sqrt{s}}\,{\rm e}^{-y_{1,2}}\,. \tag{27}$$

The allowed values of rapidities, resulting from the relations $x_{1,2}, z_{1,2}, (x_1+x_2), (z_1+z_2) \in [0,1]$, are shown in Fig. 4 (left). The solid lines correspond to constant values of (x_1+x_2) and (z_1+z_2), while the dashed lines denote constant ratios $x_2/x_1 = z_1/z_2$.

In Fig. 4 (right) we also show the DPS cross section computed using the formula (25) with factorized hard interactions

$$\frac{d^2\sigma_{W^+W^-}}{dy_1dy_2} = \frac{1}{\sigma_{\rm eff}}\frac{d\sigma_{W^+}}{dy_1}\frac{d\sigma_{W^-}}{dy_2} \tag{28}$$

where $\sigma_{\rm eff} \approx 15$ mb. The single scattering cross sections read

$$\frac{d\sigma_{W^\pm}}{dy} = \sigma_0^W \sum_{qq'} |V_{qq'}|^2 \left\{q(x_+,M_W)\,\overline{q}'(x_-,M_W) \,+\, \overline{q}(x_+,M_W)\,q'(x_-,M_W)\right\}, \tag{29}$$

where $q, \overline{q}$ are the appropriate quark/antiquark distributions, $V_{qq'}$ is the Kobayashi-Maskawa matrix and

$$\sigma_0^W = \frac{2\pi G_F}{3\sqrt{2}}\frac{M_W^2}{s}\,, \qquad\qquad x_\pm = \frac{M_W}{\sqrt{s}}\,{\rm e}^{\pm y}\,. \tag{30}$$

We used three quark flavors in the computations and the leading order MSTW08 parametrization of the SPDFs [50].

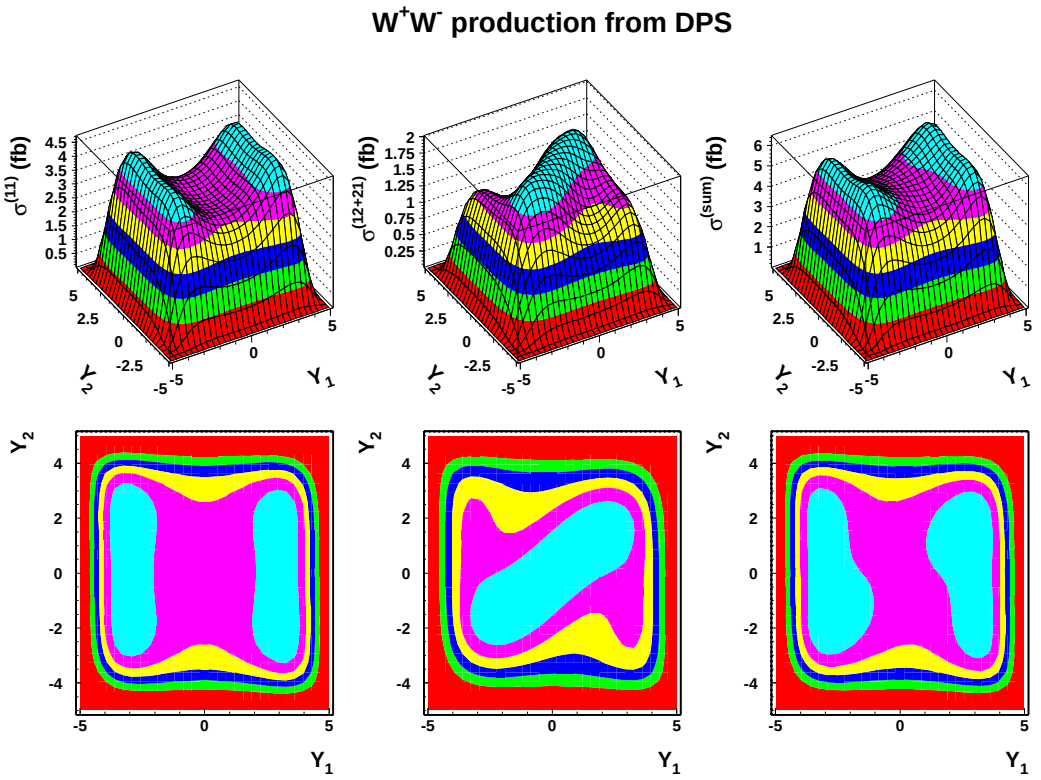

FIG. 5: The two contributions to W^+W^- production cross section (23) together with their sum (in femtobarns), differential in boson rapidities $y_{1,2}$. The contours of constant values are shown below.

To compute the DPS cross sections (23), we performed decomposition (22) with our numerical program, following the method described in Sec. III. We found the solution to the homogeneous evolution equations with the initial condition suggested in Ref. [7], $D^{(hom)}$, and the solution to the nonhomogeneous equations with zero initial conditions, $D^{(nhom)}$. The two components in Eq. (22) are written with the help of the found solutions

$$D^{(1)}(x_1, x_2, Q, \mathbf{q}) \;=\; D^{(hom)}(x_1, x_2, Q) F_{2g}^2(\mathbf{q}) \tag{31}$$

$$D^{(2)}(x_1, x_2, Q, \mathbf{q}) \;=\; D^{(nhom)}(x_1, x_2, Q) - D^{(nhom)}(x_1, x_2, |\mathbf{q}|) \tag{32}$$

where the subtraction in Eq. (32) accounts for the lower integration limit in Eq. (20).

The two contributions to the cross section $d\sigma_{AB}/dy_1 dy_2$ are shown for the W^+W^- production in Fig. 5 and for the Z^0Z^0 production in Fig. 6. We see that in both cases the single splitting contribution, $\sigma^{(12+21)}$, is comparable with the standard contribution, $\sigma^{(11)}$. Notice also that the latter contribution stays very close to the factorized form (28), see Fig. 4 (right). We quantify these observations in the next section. In Table I we present the values of these contributions to the total cross sections, obtained after the integration over the allowed values of boson rapidities.

in [fb]	$\sigma_{tot}^{(11)}$	$\sigma_{tot}^{(12+21)}$	$\sigma_{tot}^{(12+21)}/\sigma_{tot}^{(11)}$
W^+W^-	256	97	0.38
Z^0Z^0	61	22	0.36

TABLE I: Contributions to the total DPS cross sections for electroweak boson production.

Some remarks concerning the correlation pattern in rapidities are in order, especially for the W^+W^- production. The standard contribution, $\sigma^{(11)}$, is dominated by the production of the W^+ boson with rapidity $y_1 \approx \pm 4$ and the W^- boson in the broad range of the rapidity y_2. This is well understood from the factorized form (28) of the DPS cross section, given in terms of the SPS cross sections with the characteristic shapes in rapidity, see e.g. Ref. [51] for

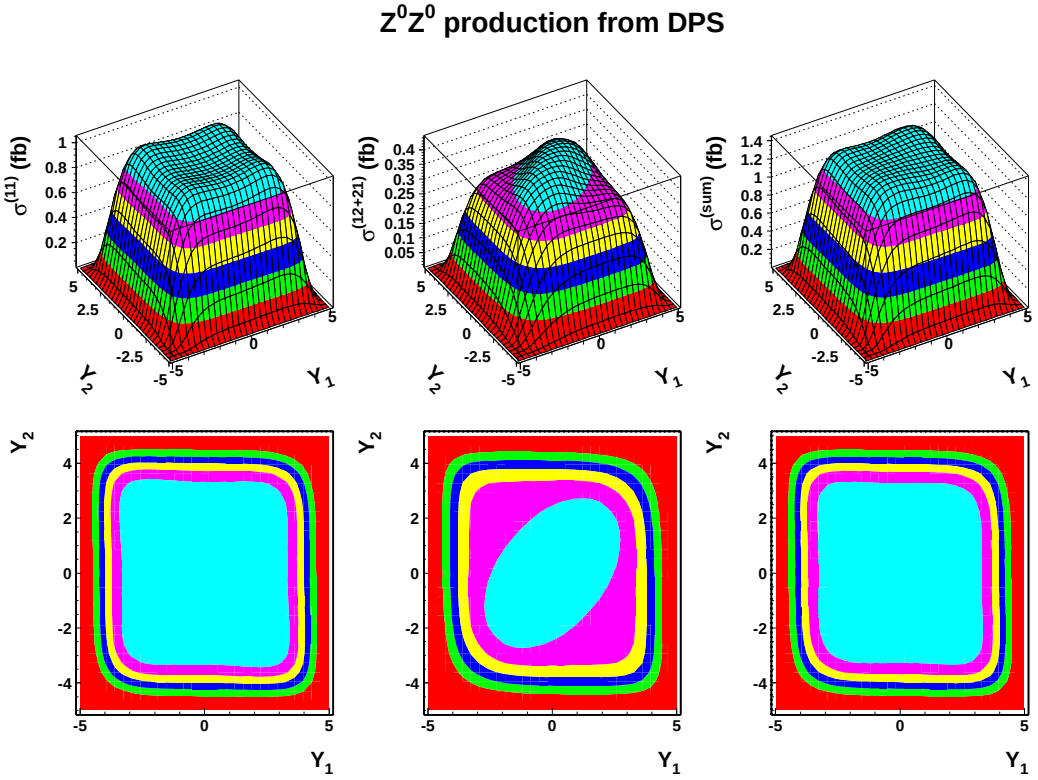

FIG. 6: The same as in Fig. 5 but for Z^0Z^0 bosons.

these shapes in the LHC kinematics. Such a pattern reflects the dominant mechanism of the W^+ production from the valence u quark with the longitudinal momentum fraction $x \approx 0.3$ which annihilates with the sea $\bar{d}$ quark. On the other hand, in the single splitting contribution, $\sigma^{(12+21)}$, the $W^\pm$ bosons are produced mostly with rapidities which are correlated along the line of equal rapidities, $y_1 = y_2$. The sum of the two contributions in Fig. 5 shows that the single splitting contribution leads to the distortion of the rapidity correlation pattern in comparison to the standard contribution correlation. We hope that this could be measured at the LHC.

VI. DISCUSSION OF THE SPLITTING CONTRIBUTION

To understand to the origin of the ratios in Table I, we plot the cross section $d\sigma_{W^+W^-}/dy_1 dy_2 d\mathbf{q}^2$ as a function of $\mathbf{q}^2$ for the indicated contributions taken at the central rapidities, $y_1 = y_2 = 0$, see Fig. 7. As expected, the (11) and $(12+21)$ contributions are suppressed for large values of q^2 because of the presence of the form factor $F_{2g}(\mathbf{q})$ to the power 4 and 2, respectively, in these contributions. We found that the dependence on $\mathbf{q}$ of the nonhomogeneous distribution $D^{(2)}$ in the contribution $(12+21)$, given Eq. (20), is negligible, which is shown by the two dashed lines in Fig. 7. Thus, the single splitting contribution integrated over $\mathbf{q}$ is proportional to the integral

$$\int \frac{d^2\mathbf{q}}{(2\pi)^2}\,\theta(Q-|\mathbf{q}|)\,F_{2g}^2(\mathbf{q}) \;=\; \frac{m_g^2}{12\pi}\,. \tag{33}$$

In this way, we find the following ratios from the $\mathbf{q}$ dependence of the two contributions for $m_g = 1.5$ GeV^2,

$$\frac{m_g^2}{28\pi} : \frac{m_g^2}{12\pi} = 1 : 2.33\,. \tag{34}$$

The significant enhancement of the single splitting contribution due to the weaker q^2-dependence caused to the presence of the nonhomogeneous component, $D^{(2)}$, is compensated by its smaller size in comparison to the homogeneous component, $D^{(1)}$. Roughly speaking, in $\sigma^{(11)}$ the DPDFs are proportional to $(x^{-\lambda})^4$ with $\lambda \sim 0.3 - 0.5$ at $x < 0.1$

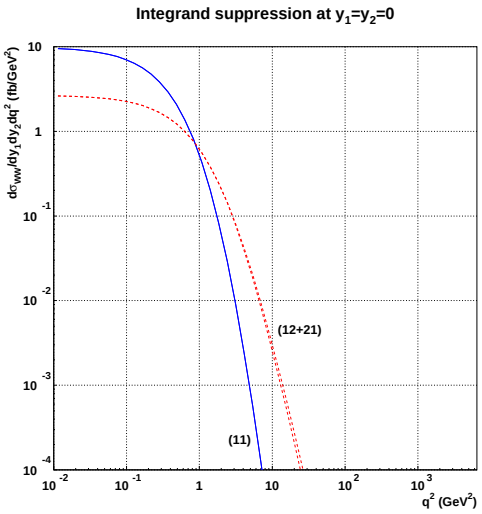

FIG. 7: The $\mathbf{q}^2$ dependence of $d\sigma_{W^+W^-}/dy_1 dy_2 d\mathbf{q}^2$ for the indicated contributions. The upper limit for $\mathbf{q}^2$ equals M_W^2.

while in $\sigma^{(12+21)}$ the DPDFs are only proportional to $(x^{-\lambda})^3$. More precisely, the ratio of the DPDFs taken for $y_1 = y_2 = 0$ in the two contributions can be found from the values of the cross sections at $\mathbf{q}^2 \approx 0$ in Fig. 7,

$$DPDF^{(11)} : DPDF^{(12+21)} = 1 : 0.27\,, \tag{35}$$

which is in reasonable agreement with the results shown in Fig. 3. Multiplying the ratios (34) and (35) we find the ratio of the differential cross sections at $y_1 = y_2 = 0$, which can be read off from Fig. 5:

$$\sigma^{(11)} : \sigma^{(12+21)} = 1 : 0.63\,. \tag{36}$$

This ratio is bigger than those for the total cross sections in Table I. Nevertheless, the mechanism explaining these ratios is all the same.

From the presented results we confirm the observation of Ref. [14] that the one splitting contribution should be considered in all analyses. We will show its significance for the estimation of the effective cross section for the electroweak boson production. Following Eq. (25), we define

$$\sigma_{\rm eff} = \frac{N}{2}\frac{(d\sigma_A/dy_1)(d\sigma_B/dy_2)}{d\sigma_{AB}/dy_1 dy_2} \tag{37}$$

for the two cases: $\sigma_{AB} = \sigma_{AB}^{(11)}$ and $\sigma_{AB} = \sigma_{AB}^{(11)} + \sigma_{AB}^{(12+21)}$. Obviously, $\sigma_{\rm eff}$ will depend on boson rapidities (y_1, y_2), which dependence illustrates the violation of a simple-minded assumption that the DPS cross section is proportional to the product of the SPS cross sections.

In Figs. 8 and 9 we show $\sigma_{\rm eff}$ for the W^+W^- and Z^0Z^0 production, respectively, in the two cases specified above, in units of the standard value of the effective cross section, $\sigma_{\rm eff} \simeq 15$ mb. For better visibility, we cut the maximal values to 1.6 or 1.2 at the edges of the phase space. We see that with the standard contribution to the DPS cross section, the factorization property is to good approximation valid in the central region of rapidities (small values of parton momentum fractions, see Fig. 4 for the correspondence). However, approaching kinematic boundaries $x_1 + x_2 = z_1 + z_2 = 1$ with comparable momentum fractions, the violation of factorization becomes stronger. This picture changes after adding the one splitting contribution. Now, the violation of factorization is significant even in the central rapidity region. The effective cross section is smaller than 15 mb, in between 60%-80% of this value (9-12 mb).

VII. SUMMARY

We have analyzed the DPS processes in the collinear approximation, using evolution equations (3) for the DPDFs. We have concentrated on the significance of the splitting terms in these equations for the DPS processes with a large hard scale $Q \sim 100$ GeV. For the illustration, we considered W^+W^- and Z^0Z^0 boson production at the LHC

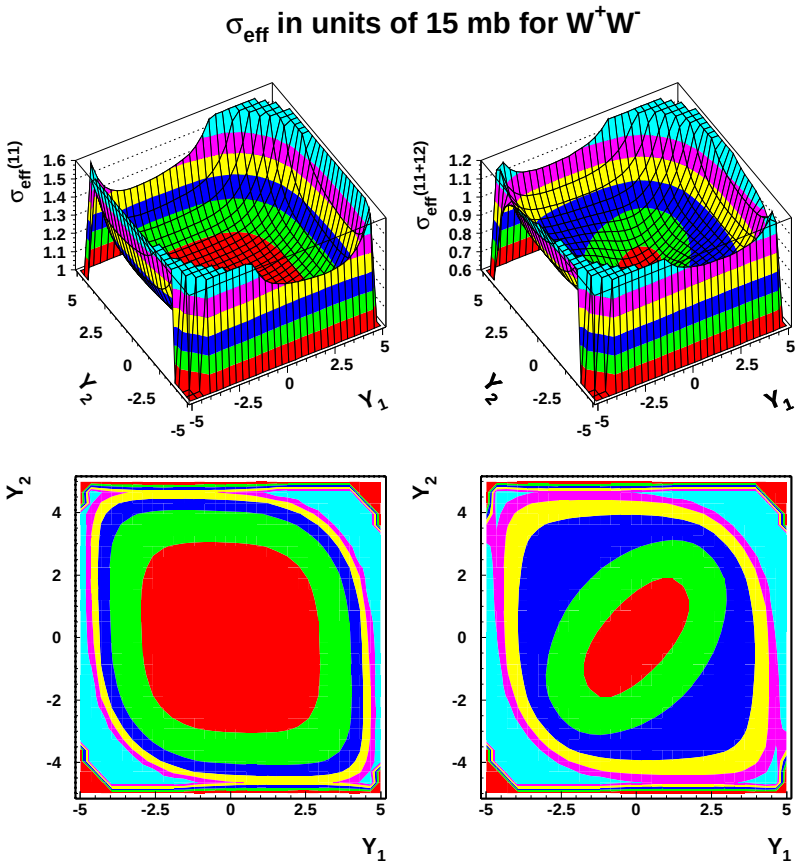

FIG. 8: $\sigma_{\rm eff}$ in units of 15 mb for W^+W^- production as a function of (y_1, y_2) for $\sigma_{AB} = \sigma_{AB}^{(11)}$ (left) and $\sigma_{AB} = \sigma_{AB}^{(11)} + \sigma_{AB}^{(12+21)}$ (right). The lines of constant values are shown below.

center-of-mass energy 14 TeV. To compute the DPS cross sections, we have specified the dependence of the DPDFs on the relative momentum $\mathbf{q}$, following Ref. [12]. In this model, the splitting component of the DPDFs is not strongly suppressed at large values of the relative momentum fraction $|\mathbf{q}|$, like the standard component, because it originates from the splitting of a pointlike parton. Based on the constructed numerical program which solves the evolution equations for DPDFs, we analyzed the single splitting contribution to the DPS cross sections for the electroweak boson production. We quantified the relevance of the single splitting contribution in such a case in terms of the effective cross section. We also discussed correlations in rapidity for the produced $W^\pm$ bosons pointing out that the single splitting contribution distorts the standard correlation obtained with the factorized DPS cross section.

Note added in proof - Once the first version of this paper was released we found that Ref. [52] appeared which addresses the same problems but for different DPS cross sections, using the same methods.

Acknowledgments

This work was supported by the Polish NCN Grant No. DEC-2011/01/B/ST2/03915 and by the Center for Innovation and Transfer of Natural Sciences and Engineering Knowledge in Rzeszów.

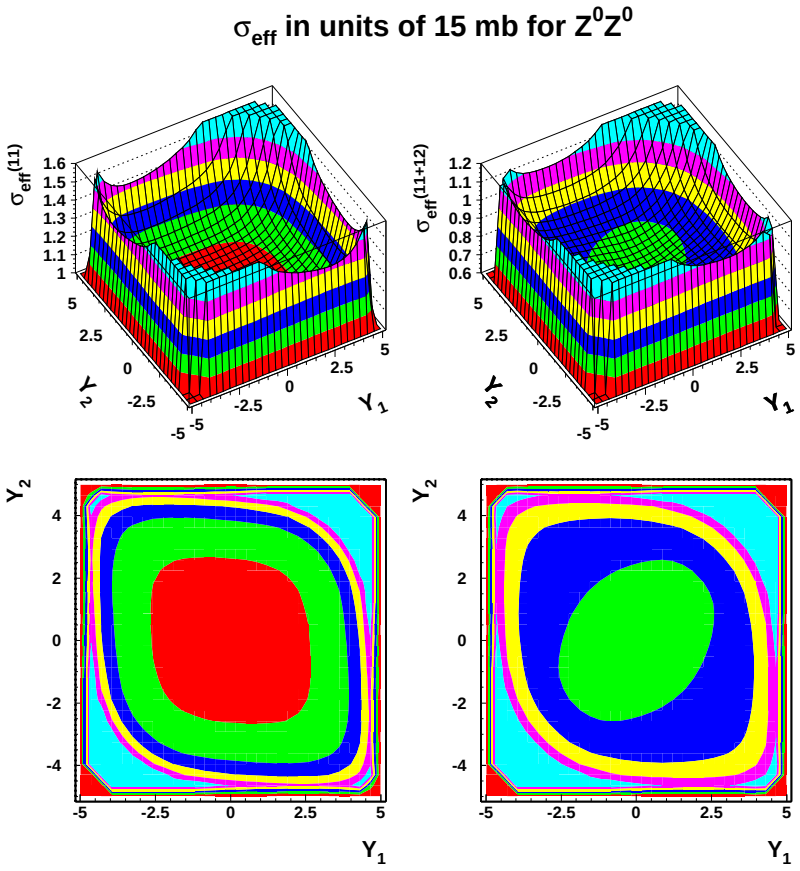

FIG. 9: The same as in Fig. 8 but for Z^0Z^0 production.

VIII. REFERENCES

[1] V. Shelest, A. Snigirev and G. Zinovev, Phys.Lett. **B113**, 325 (1982).
[2] G. Zinovev, A. Snigirev and V. Shelest, Theor.Math.Phys. **51**, 523 (1982).
[3] R. K. Ellis, W. Furmanski and R. Petronzio, Nucl.Phys. **B212**, 29 (1983).
[4] A. Bukhvostov, G. Frolov, L. Lipatov and E. Kuraev, Nucl.Phys. **B258**, 601 (1985).
[5] A. M. Snigirev, Phys. Rev. **D68**, 114012 (2003), [hep-ph/0304172].
[6] V. L. Korotkikh and A. M. Snigirev, Phys. Lett. **B594**, 171 (2004), [hep-ph/0404155].
[7] J. R. Gaunt and W. J. Stirling, JHEP **03**, 005 (2010), [0910.4347].
[8] B. Blok, Y. Dokshitzer, L. Frankfurt and M. Strikman, Phys.Rev. **D83**, 071501 (2011), [1009.2714].
[9] F. A. Ceccopieri, Phys. Lett. **B697**, 482 (2011), [1011.6586].
[10] M. Diehl and A. Schafer, Phys. Lett. **B698**, 389 (2011), [1102.3081].
[11] J. R. Gaunt and W. J. Stirling, JHEP **1106**, 048 (2011), [1103.1888].
[12] M. Ryskin and A. Snigirev, Phys.Rev. **D83**, 114047 (2011), [1103.3495].
[13] J. Bartels and M. G. Ryskin, 1105.1638.
[14] B. Blok, Y. Dokshitser, L. Frankfurt and M. Strikman, Eur.Phys.J. **C72**, 1963 (2012), [1106.5533].
[15] M. Diehl, D. Ostermeier and A. Schafer, JHEP **1203**, 089 (2012), [1111.0910].
[16] A. V. Manohar and W. J. Waalewijn, Phys.Rev. **D85**, 114009 (2012), [1202.3794].
[17] M. Ryskin and A. Snigirev, Phys.Rev. **D86**, 014018 (2012), [1203.2330].
[18] J. R. Gaunt, JHEP **1301**, 042 (2013), [1207.0480].
[19] A. Snigirev, N. Snigireva and G. Zinovjev, Phys.Rev. **D90**, 014015 (2014), [1403.6947].
[20] T. Sjostrand and M. van Zijl, Phys.Rev. **D36**, 2019 (1987).

[21] A. Del Fabbro and D. Treleani, Phys. Rev. **D61**, 077502 (2000), [hep-ph/9911358].
[22] A. Kulesza and W. J. Stirling, Phys.Lett. **B475**, 168 (2000), [hep-ph/9912232].
[23] A. Del Fabbro and D. Treleani, Phys. Rev. **D66**, 074012 (2002), [hep-ph/0207311].
[24] E. Cattaruzza, A. Del Fabbro and D. Treleani, Phys. Rev. **D72**, 034022 (2005), [hep-ph/0507052].
[25] T. Sjostrand and P. Z. Skands, JHEP **0403**, 053 (2004), [hep-ph/0402078].
[26] E. L. Berger, C. Jackson and G. Shaughnessy, Phys.Rev. **D81**, 014014 (2010), [0911.5348].
[27] J. R. Gaunt, C.-H. Kom, A. Kulesza and W. J. Stirling, Eur. Phys. J. **C69**, 53 (2010), [1003.3953].
[28] A. Snigirev, Phys.Rev. **D81**, 065014 (2010), [1001.0104].
[29] C. Kom, A. Kulesza and W. Stirling, Phys.Rev.Lett. **107**, 082002 (2011), [1105.4186].
[30] E. L. Berger, C. Jackson, S. Quackenbush and G. Shaughnessy, Phys.Rev. **D84**, 074021 (2011), [1107.3150].
[31] C. Kom, A. Kulesza and W. Stirling, Eur.Phys.J. **C71**, 1802 (2011), [1109.0309].
[32] P. Bartalini *et al.*, 1111.0469.
[33] M. Luszczak, R. Maciula and A. Szczurek, Phys.Rev. **D85**, 094034 (2012), [1111.3255].
[34] D. d'Enterria and A. M. Snigirev, Phys.Lett. **B718**, 1395 (2013), [1211.0197].
[35] D. d'Enterria and A. M. Snigirev, Phys.Lett. **B727**, 157 (2013), [1301.5845].
[36] R. Maciula and A. Szczurek, Phys.Rev. **D87**, 074039 (2013), [1301.4469].
[37] Axial Field Spectrometer Collaboration, T. Akesson *et al.*, Z.Phys. **C34**, 163 (1987).
[38] CDF Collaboration, F. Abe *et al.*, Phys.Rev.Lett. **79**, 584 (1997).
[39] CDF Collaboration, F. Abe *et al.*, Phys.Rev. **D56**, 3811 (1997).
[40] D0 Collaboration, V. Abazov *et al.*, Phys.Rev. **D81**, 052012 (2010), [0912.5104].
[41] ATLAS Collaboration, G. Aad *et al.*, New J.Phys. **15**, 033038 (2013), [1301.6872].
[42] CMS Collaboration, S. Chatrchyan *et al.*, JHEP **1403**, 032 (2014), [1312.5729].
[43] ATLAS Collaboration, G. Aad *et al.*, JHEP **1404**, 172 (2014), [1401.2831].
[44] M. W. Krasny and W. Placzek, Acta Phys.Polon. **B45**, 71 (2014), [1305.1769].
[45] R. Kirschner, Phys.Lett. **B84**, 266 (1979).
[46] A. Snigirev, Phys.Atom.Nucl. **74**, 158 (2011).
[47] K. Golec-Biernat and E. Lewandowska, to be publihsed .
[48] W. H. Press, S. A. Teukolsky, W. T. Vetterling and B. P. Flannery, ISBN-9780521430647.
[49] A. V. Manohar and W. J. Waalewijn, Phys.Lett. **B713**, 196 (2012), [1202.5034].
[50] A. Martin, W. Stirling, R. Thorne and G. Watt, Eur.Phys.J. **C63**, 189 (2009), [0901.0002].
[51] K. Golec-Biernat and A. Luszczak, Phys.Rev. **D81**, 014009 (2010), [0911.2789].
[52] J. R. Gaunt, R. Maciula and A. Szczurek, Phys.Rev. **D90**, 054017 (2014), [1407.5821].